



Published in final edited form as:

Circulation. 2018 February 06; 137(6): 605–618. doi:10.1161/CIRCULATIONAHA.117.028976.

Increased cardiac arrhythmogenesis associated with gap junction remodeling with upregulation of RNA binding protein FXR1

Mienscheng Chu, PhD^{*,1}, Stefanie Mares Novak, PhD^{*,1}, Cathleen Cover, BS¹, Anne A. Wang, BS¹, Ikeotunye Royal Chinyere, BS², Elizabeth B. Juneman, MD², Daniela C. Zarnescu, PhD³, Pak Kin Wong, PhD⁴, and Carol C. Gregorio, PhD¹

¹Department of Cellular and Molecular Medicine and Sarver Molecular Cardiovascular Research Program, University of Arizona, Tucson, AZ

²Department of Medicine, University of Arizona, Tucson, AZ

³Department of Molecular and Cellular Biology at the University of Arizona, Tucson, AZ

⁴Department of Biomedical Engineering at Pennsylvania State University, University Park, PA

Abstract

Background—Gap junction remodeling is well established as a consistent feature of human heart disease involving spontaneous ventricular arrhythmia. The mechanisms responsible for gap junction remodeling that include alterations in the distribution of, and protein expression within, gap junctions are still debated. Studies reveal that multiple transcriptional and post-transcriptional regulatory pathways are triggered in response to cardiac disease, such as those involving RNA-binding proteins. The expression levels of Fragile × mental retardation autosomal homolog 1 (FXR1), an RNA-binding protein, are critical to maintain proper cardiac muscle function; however, the connection between FXR1 and disease is not clear.

Methods—To identify the mechanisms regulating gap junction remodeling in cardiac disease, we sought to identify: the functional properties of FXR1 expression, direct targets of FXR1 in human left ventricle dilated cardiomyopathy (DCM) biopsy samples and mouse models of DCM through BioID proximity assay and RNA immunoprecipitation, how FXR1 regulates its targets through RNA stability and luciferase assays, and functional consequences of altering the levels of this important RNA binding protein through the analysis of cardiac-specific FXR1 knockout mice and mice injected with 3xMyc-FXR1 adeno-associated virus.

Results—FXR1 expression is significantly increased in tissue samples from human and mouse models of DCM via western blot analysis. FXR1 associates with intercalated discs and integral gap junction proteins Cx43, Cx45 and ZO-1 were identified as novel mRNA targets of FXR1 using a BioID proximity assay and RNA immunoprecipitation. Our findings show FXR1 is a

Send correspondence to: Carol C. Gregorio, PhD, Dept. of Cellular and Molecular Medicine, The University of Arizona, 1656 East Mabel, Tucson AZ 85724, gregorio@email.arizona.edu, TEL (520) 626-8113.

*Equal contribution as first authors.

Disclosures

None

multifunctional protein involved in translational regulation and stabilization of its mRNA targets in heart muscle. Additionally, introduction of 3xMyc-FXR1 via adeno-associated virus into mice leads to redistribution of gap junctions and promotes ventricular tachycardia showing functional significance of FXR1 upregulation observed in DCM.

Conclusions—In DCM, increased FXR1 expression appears to play an important role in disease progression by regulating gap junction remodeling. Together this study provides a novel function of FXR1 namely that it directly regulates major gap junction components, contributing to proper cell-cell communication in the heart.

Keywords

FXR1; gap junction; ZO-1; Cx43; cardiac muscle

INTRODUCTION

Ventricular arrhythmias in patients with dilated cardiomyopathy (DCM) results in an increased risk for sudden cardiac death.¹ In DCM, alterations in cell-cell connections at intercalated discs compromise the structural integrity of the heart (for review²). Connections at the intercalated disc consist of three complexes: fascia adherens and desmosomes that anchor cardiomyocytes together, and gap junctions that allow for cell-cell communication. Contributing to arrhythmogenesis are alterations in the distribution of, and protein expression within, gap junctions that allow chemical and electrical coupling between cardiomyocytes – a process known as gap junction remodeling (for review³). Downregulation of connexin 43 (Cx43), the predominant connexin expressed in ventricles is a typical feature of gap junction remodeling linked to development of arrhythmias in human cardiomyopathies.^{4–6} Several proteins have been implicated in gap junction remodeling process such as zonula occludens-1 (ZO-1) (for review⁷). ZO-1 localizes to the intercalated disc where it regulates the organization of gap junctions and adherens junctions (e.g.,⁸). ZO-1 directly interacts with Cx43 and affects Cx43 expression and gap junction plaque size.^{9–11} Interestingly, upregulation of ZO-1 protein levels are also seen in human dilated and ischaemic cardiomyopathies.¹¹ The mechanism regulating Cx43 and ZO-1 expression during cardiac disease progression is still undefined.

Dysregulation of RNA-binding proteins is implicated in many diseases including cardiomyopathies, cancers, neurological disorders and muscular atrophies (for review¹²). Important in cardiac development and disease is the RNA binding protein, Fragile × mental retardation syndrome-related protein 1 (FXR1).^{13–15} FXR1 is a member of the Fragile × family of RNA-binding proteins (FraX) which includes FMRP, FXR1 and FXR2. FraX members can form hetero- and homodimers, as well as larger complexes with additional proteins.¹⁶ Each member contains three RNA-binding domains (two KH-domains; one RGG-box). The RNA-recognition element for the KH domain can bind kissing complex RNA motifs while the RGG box recognizes G-quadruplexes.^{17,18} Both of these RNA-binding domains allow FraX members to control expression of an assortment of mRNA targets.

Previous studies primarily focused on FMRP since absence of, or mutations in, FMRP leads to Fragile × Syndrome; this is the most common form of inherited mental retardation and autism in humans. FXR1 is the only isoform with robust expression in striated muscle, where it localizes to puncta in the cytosol and is enriched at Z-discs (border of sarcomeres).^{13,19} Ablation of *Fxr1* in mice results in perinatal lethality most likely due to cardiac defects, while a reduction of FXR1 protein expression in zebrafish results in cardiomyopathy.^{13–15} FXR1 has been shown to directly regulate various transcripts (i.e., desmoplakin, talin2, TNF α and p21), in addition to interacting with the microRNA pathway (via Dicer and Argonaute2 binding), supporting its role as an important regulator in the heart.^{15,20–23} Despite the essential importance of FXR1 in cardiac function, surprisingly few direct targets have been identified.

To test our hypothesis that FXR1 is an important regulator of gap junction downregulation in human cardiomyopathy, FXR1 expression in human left ventricle DCM biopsy samples was examined and assessed for its role in regulating levels of prominent gap junction components. FXR1 expression is significantly increased in human DCM samples, and in mouse models of DCM. FXR1 associates with intercalated disc, directly interacts with Cx43, Cx45 and ZO-1 mRNA and can regulate Cx43, Cx45 and ZO-1 protein levels via translational regulation and mRNA stability. Furthermore, upregulation of FXR1 in the heart promotes redistribution of gap junctions and subsequently regulates ventricular tachycardia in mice. While loss of FXR1 in the heart leads to DCM, no change in Cx43 expression is observed, as is observed in hearts from other DCM models. Taken together, we demonstrate FXR1 directly regulates critical gap junction proteins and maintains cardiac conduction. We provide a potential mechanism of ventricular arrhythmias, whereby gap junction remodeling is directly regulated by FXR1.

METHODS

An expanded Methods section is available in Supplemental Materials. The data and methods will be made available to other researchers for purposes of reproducing the results or replicating the procedure via email contact with the Corresponding author.

Tissue from Non-failing and Failing Human Hearts

Well-characterized samples of left ventricle (LV) tissue from patients with non-failing (NF) or failing (non-ischaemic dilated cardiomyopathy) hearts were obtained from Loyola University Health System (LUHS) Cardiovascular Institute Tissue Repository and Gift of Hope Organ and Tissue Donor Network as published.^{24–27} Following institutional review committee approval from LUHS and University of Arizona, as well as informed consent from organ donor family members or patients undergoing heart transplantation, tissue samples were surgically removed, frozen in liquid N₂, and stored at –80°C.

Mouse models

Lmod2 knockout mice are in C57BL/6J background²⁸; samples used for immunoblotting were collected from 19 day-old mice. MLP knockout mice are in a mixed SV129/Black Swiss background²⁹; samples used for immunoblotting were collected from two-month-old

male mice. Conditional FXR1 knockout mice (*fxr1^{f/f}*) were obtained from Baylor College of Medicine and crossed onto Myh6-Cre knock-in line for cardiac-specific knockout. Mice were maintained in accordance with institutional guidelines and procedures approved by Institutional Animal Care and Use Committee at the University of Arizona.

Statistics

A student's t-test was used to determine significance for protein and mRNA levels in human and mouse samples, and for gap junction plaque size and Cx43 localization. For luciferase assay, a student's t-test was used to compare each individual luciferase construct between treatment groups. To determine statistical significance, a one-way ANOVA with post-hoc Tukey was used for protein and mRNA levels in cardiomyocytes, a two-way ANOVA with post-hoc Bonferroni was used for the polysome assay, a two-way repeated-measures ANOVA with post-hoc Bonferroni was used for the RNA stability assay, and an unpaired t-test was used to analyze statistical difference in presence or absence of ventricular tachycardia between groups.

RESULTS

FXR1 protein is upregulated in human and mouse models of dilated cardiomyopathy

To assess FXR1's role in human cardiac disease, we quantitatively analyzed FXR1 protein expression levels in biopsies from patients with dilated cardiomyopathy (DCM). We found that FXR1 protein is significantly increased (1.61 ± 0.231 , $p < 0.05$) in left ventricles from DCM patients, with no change in FXR1 mRNA detected (data shown for protein in Figure 1A,B). These results suggest that FXR1 protein expression levels are linked to human DCM disease.

To determine whether FXR1 upregulation contributes to development of dilated cardiomyopathy and whether FXR1 is a common feature of cardiomyopathies, we studied MLP (muscle LIM protein) knockout mice that are among the most extensively characterized mouse model for DCM and display ventricular chamber enlargement at 2 months (e.g.,²⁹). FXR1 levels were also investigated in LMOD2 (Leiomodin 2) knockout mice, which we reported display a rapid ventricular chamber enlargement consistent with dilated cardiomyopathy clearly evident at day 15 but die shortly after as juveniles.²⁸ Quantification of FXR1 protein levels in LV tissue samples from MLP (Figure 1C,D) and LMOD2 KO (Figure 1E,F) mice compared with wild type controls revealed that FXR1 protein is significantly increased (MLP KO: 3.05 ± 0.343 , $p < 0.0001$; LMOD2 KO: 2.29 ± 0.335 , $p < 0.01$) in both models of DCM, indicating that FXR1 upregulation is a common feature of DCM.

FXR1 localizes with intercalated discs

To determine if FXR1 functions at the intercalated disc, a BioID proximity assay was performed to identify whether FXR1 interacts with any proteins in this cellular location. A MycBirA*-FXR1 fusion protein was expressed in neonatal cardiomyocytes. Expression of full-length fusion protein (Figure 2A) and overall enrichment of biotinylated proteins (Figure 2B) were confirmed. To identify novel protein interactors, a BioID pull-down was

performed and candidate proteins were identified by Western blot analysis. ZO-1 and N-cadherin were identified as potential interactors of FXR1 (Figure 2C), suggesting FXR1 may be functionally associated with intercalated discs.

Previous studies reported that FXR1 localizes to puncta in the cytosol (e.g., associated with stress granules³⁰) and is enriched at Z-discs (border of sarcomeres).^{13,19} To determine if FXR1 also localizes to intercalated discs, immunofluorescence imaging on adult mice LV tissue sections was performed. FXR1 localized to cytosolic puncta and enriched at most intercalated discs when co-stained for plakoglobin, a marker of intercalated discs (Figure 2D). This localization at intercalated discs is consistent with our previous report that FXR1 regulates the expression of the desmosomal protein desmoplakin in cardiomyocytes.¹⁵

FXR1 directly interacts with Cx43, Cx45 and ZO-1 mRNAs

Altered structural integrity in DCM commonly leads to changes in composition and structure of the intercalated disc, in particular gap junction remodeling, leading to increased arrhythmogenic risk (e.g.,³¹). To investigate if FXR1 regulates the integrity of gap junctions, we determined whether mRNAs encoding any major gap junction proteins of the LV are targets of FXR1. Fragile × family members interact with nucleotide sequences capable of forming G-quadruplexes. QGRS Mapper was used for predicting G-quadruplexes in nucleotide sequences in the primary gap junction proteins: Cx43, Cx45 and ZO-1 mRNA sequences.³² We also examined G-quadruplexes in additional intercalated disc proteins: desmoplakin, a FXR1 mRNA target¹⁵ as well as N-cadherin, identified as a potential protein interactor of FXR1 in the BioID pull-down assay (Figure 2C) and as a protein involved in formation and/or function of gap junctions (e.g.,³³). The results show that a majority of G-quadruplexes are located within the coding region of Cx43, Cx45, ZO-1, N-cadherin and desmoplakin mRNA (Supplemental Table 1), suggesting these mRNAs may interact with (and be regulated by) FXR1.

To determine if Cx43, Cx45 and/or ZO-1 mRNA are indeed present in the FXR1 RNA-IP complex, an RNA-IP was performed to isolate FXR1 protein-RNA complexes from non-failing human LV tissue (Figure 3A). End-point PCR was used to detect transcripts whose cognate proteins are major constituents of gap junctions in the LV (see Supplemental Table 2 for primers). Cx43, Cx45 and ZO-1 mRNA transcripts are reproducibly identified in FXR1 RNA-IPs (Figure 3D). Little to no signal is detected in IgG IP control, indicating that amplification is specific for RNA associated with FXR1. Next, FXR1 protein-RNA complexes were isolated from adult mouse heart tissue (Figure 3B), and cultured rat cardiomyocytes (Figure 3C); Cx43, Cx45 and ZO-1 mRNA are present in the FXR1 protein-RNA complex (Figure 3E–F). To determine if these interactions with FXR1 are direct, a direct binding assay was performed. Based on predicted G-quadruplex results, coding sequences of Cx43, Cx45 and ZO-1 mRNAs were synthesized by *in vitro* transcription, labeled with biotin, and incubated with recombinant FXR1. At 50–150pmol of transcript, FXR1 protein binds directly to Cx43, Cx45 and ZO-1 but not β 2M mRNA (negative control) (Figure 3G). Thus, FXR1 can directly bind to Cx43, Cx45 and ZO-1 mRNA, allowing for possible post-transcriptional regulation of gap junction remodeling.

FXR1 regulates Cx43 and ZO-1 protein expression

FXR1 plays a critical role in translational regulation by interacting with target mRNAs. Since FXR1 interacts with mRNAs encoding major gap junction proteins, it was determined whether FXR1 regulates their protein expression. Primary rat cardiomyocytes were transduced with different multiplicity of infections (MOIs) of FXR1 or β -gal adenovirus. Western blot analysis confirmed increased expression of FXR1 protein ranging from 5–10 fold in cells transduced with FXR1 adenovirus (Figure 4A–B). Cx43 is significantly repressed in a dose-dependent manner in response to increased FXR1 expression levels (Figure 4A,C). Next, it was determined whether alterations in protein levels of Cx43 are due to effects on transcript levels. RT-PCR showed that Cx43 mRNA is significantly reduced in cells with increased FXR1 (10 MOI: $33.37 \pm 4.55\%$ of control, $p < 0.01$; 20 MOI: $36.71 \pm 7.89\%$ of control, $p < 0.001$; Supplemental Figure 1A). The discovery that Cx43 mRNA is altered could explain the reduction in protein. Alternatively, FXR1 could regulate Cx43 through both transcriptional and translational mechanisms.

Several studies show ZO-1 plays a critical role in gap junction organization by interacting with Cx43 protein. Since FXR1 interacts with ZO-1 protein and mRNA (Figures 2C,3), whether ZO-1 protein levels are also regulated by FXR1 was investigated. Interestingly, in neonatal rat cardiomyocytes transduced with different MOIs of FXR1, ZO-1 levels are significantly increased at low levels (10 MOI) and reduced at high levels of FXR1 expression (20 MOI) (Figure 4A,D). Alterations in protein levels of ZO-1 are due to effects at the transcript level. RT-PCR showed that ZO-1 mRNA levels are not changed (Supplemental Figure 1B) suggesting FXR1 regulates ZO-1 through a translational mechanism.

Upregulation of Cx45 has been reported in heart failure patients (i.e., those with dilated or ischemic cardiomyopathy), possibly compensating for reduced Cx43 levels.³⁴ Therefore, Cx45 protein and mRNA levels in neonatal rat cardiomyocytes overexpressing FXR1 were analyzed. Interestingly, while Cx45 protein levels are unchanged (Figure 4E–F), Cx45 mRNA levels are increased in rat cardiomyocytes transduced with different MOIs of FXR1 (Supplemental Figure 1C). These results suggest that FXR1 may regulate Cx45 by stabilizing its mRNA and/or by a transcriptional mechanism. Another possibility is that FXR1 may repress the translation of the elevated Cx45 transcript to maintain Cx45 protein expression. To test whether other intercalated disc proteins are affected by FXR1 overexpression, we analyzed expression of N-cadherin and plakoglobin. Both proteins are not altered upon FXR1 overexpression (Supplemental Figure 2). These results are consistent with the hypothesis that changes observed specifically in gap junction remodeling are due to FXR1.

Since FXR1 upregulation alters Cx43 and ZO-1 expression, these proteins were further studied in human DCM LV tissue samples. In human samples Cx43 protein expression is significantly reduced (0.43 ± 0.076 of non-failing control, $p < 0.001$) while ZO-1 protein levels are unchanged (Supplemental Figure 3). In MLP-KO mice Cx43 protein expression is significantly reduced (0.62 ± 0.041 of WT control, $p < 0.01$) similarly to previously shown³⁵, while interestingly, ZO-1 protein is significantly increased (2.22 ± 0.271 of WT control, $p < 0.001$) (Supplemental Figure 4). In Lmod2-KO mice LV samples Cx43 protein expression

is surprisingly not changed; yet ZO-1 protein is significantly increased (3.61 ± 0.517 of WT control, $p < 0.001$) (Supplemental Figure 5). Although upregulation of ZO-1 is not consistent with the human DCM samples, it is consistent with the cardiomyocyte data where we altered the expression levels of FXR1 showing the lower dose (5-fold increase of FXR1) results in increased ZO-1 expression. Overall these data reveal that elevated FXR1 levels in DCM can contribute to the regulation of major gap junction proteins by multiple transcriptional and translation mechanisms depending on the specific target it is regulating.

FXR1 is involved in translational regulation and mRNA stability

To examine whether FXR1 controls Cx43, Cx45 and ZO-1 through translational regulation, polysome fractionation was performed from cardiomyocytes transduced with 10 MOI of FXR1 or β -gal adenovirus. Western blot analysis shows FXR1 associates with both untranslated fractions (RNPs and ribosomal subunits) and actively translating polyribosomes (Figure 5A). Overexpression of FXR1 causes a slight increase in FXR1 protein associated with the heavy polysome fraction (i.e., actively translating fraction) compared with HuR, which does not change its distribution (Figure 5B). These results are consistent with FXR1 being involved in translational regulation. Consequently, if FXR1 regulates its mRNA target translation, polysome fractionation could show either a shift in the target mRNA associated with heavy polysome fraction or change in total target mRNA in the polysome fraction. To determine the distribution of Cx43, Cx45 and ZO-1, each fraction from the gradient was analyzed by RT-PCR. Cx43 mRNA distribution is not changed upon FXR1 overexpression (Supplemental Figure 6B) but there is a decrease in total Cx43 mRNA in the polysome fraction (Figure 5C). On the contrary, there is a reduction in ZO-1 mRNA in the actively translating polysome fraction upon FXR1 overexpression (Supplemental Figure 6C) but no change in total ZO-1 mRNA levels in the polysome fraction (Figure 5C). No change was observed in Cx45 mRNA distribution and its total levels in the polysome fraction (Figure 5C; Supplemental Figure 6D).

To further confirm if FXR1 regulates translation of Cx43, Cx45 and ZO-1, we used an *in vitro* dual luciferase assay. In this assay, coding sequences of Cx43, Cx45 and ZO-1 mRNA were inserted downstream of a pMirGLO dual-luciferase vector (pMir) and co-transfected with shFXR1 to knockdown FXR1 expression or shLuc (control) into C2C12 cells. Transfection efficiency and cell viability were monitored using *Renilla* luciferase, and data reported as Firefly:*Renilla* ratios normalized to pMir for each sample. Luciferase activity is significantly reduced for Cx43 in cells expressing FXR1 (65.2% of shLuc compared to shFXR1, $p < 0.05$; Figure 5D). No change was seen for ZO-1 and Cx45 in cells expressing FXR1 (Figure 5D). These results demonstrate that FXR1 regulates translation of Cx43, but may regulate ZO-1 and Cx45 through other mechanisms.

Although no change was seen in Cx45 protein expression, an increase in Cx45 mRNA was seen upon FXR1 overexpression (Supplemental Figure 1). To determine whether Cx45 is regulated transcriptionally via stabilization of its RNA, we performed RNA stability assays on rat cardiomyocytes treated with actinomycin D to block transcription. RNA was isolated after 0, 3, 6 or 12hrs and the levels of Cx43, Cx45 and ZO-1 mRNAs were measured by RT-PCR. Cx45 and ZO-1 mRNAs are significantly more stable in cardiomyocytes

overexpressing FXR1 ($T_{1/2}$ Cx45=4.5h, ZO-1=9.3h), compared with control cardiomyocytes overexpressing β -gal ($T_{1/2}$ Cx45=2.7h, ZO-1=3.3h) (Supplemental Figure 7). Conversely, Cx43 mRNA stability is not changed between the two groups. Together, these results indicate that FXR1 can regulate Cx45 and ZO-1 but not Cx43 mRNA stability.

Gap junction plaque size is reduced when FXR1 levels are elevated

In DCM, gap junction remodeling includes a decrease in Cx43 expression and a reduction in gap junction plaque size.¹¹ Increased expression of FXR1 in neonatal rat cardiomyocytes leads to a significant reduction in Cx43 protein (Figure 4C). To examine gap junction plaque size, immunofluorescence imaging was performed. Cardiomyocytes were plated on patterned plates to enhance cell-to-cell contact and gap junction formation. Immunofluorescence staining of Cx43 shows visibly smaller gap junction plaques (Figure 5F). Quantification of plaques confirmed that gap junction plaques are on average smaller in cells expressing increased levels of FXR1 ($22.29 \pm 0.605\%$, $p < 0.001$) versus β -gal control (Figure 5E). This result supports our hypothesis that FXR1 translationally represses Cx43 protein leading to reduction in gap junction plaque size.

FXR1 overexpression in mice promotes gap junction redistribution plus ventricular tachycardia

To better understand the role of FXR1 in gap junction remodeling *in vivo*, we increased the levels of FXR1 in hearts of C57BL/6 mice via injection of 3xMyc-FXR1 adeno-associated virus (AAV). With a significant increase in FXR1 protein (7.33 ± 1.62 , $p < 0.01$), Cx43 protein expression is significantly reduced (0.81 ± 0.028 , $p < 0.05$) with no change in Cx43 mRNA; this result is consistent with that observed with elevated FXR1 levels in neonatal cardiomyocytes (data shown for protein in Figures 6A–C). No change was observed for both ZO-1 and Cx45 protein and mRNA levels (data shown for protein in Figures 6A,D–E). Immunofluorescence analysis confirmed a 29.7% reduction in Cx43 at the intercalated disc (as marked by presence of plakoglobin) in left ventricle sections from 3xMyc-FXR1 AAV injected mice (Figure 7C–D). >50% of cells that were enriched for FXR1 show variable levels of redistribution of Cx43 to lateral interfaces between cardiomyocytes (Figure 7D). This significant change in distribution of Cx43 is predicted to enhance reentry circuits in the myocardium that enable ventricular tachycardia.

Echocardiography and electrophysiological (EP) studies were performed on the transduced mice. Echocardiography shows no functional difference between 3xMyc-FXR1 AAV-injected and control mice (Supplemental Figure 8). Upon programmed electrical stimulation FXR1 transduced mice had inducible ventricular tachycardia (100%) whereas control mice did not (0%) ($p < 0.05$) (Figure 7A,B). These data suggest FXR1 expression level is critical to maintain proper gap junction protein expression and assembly in cardiomyocytes. Misregulation of FXR1 *in vivo* can augment the gap junction remodeling in cardiac disease and contribute to myocardial electrical abnormalities.

Cardiac-specific loss of FXR1 leads to DCM

To determine whether FXR1 regulates gap junction remodeling in DCM, a conditional loss-of-function approach was taken, using a floxed *fxr1* allele (*fxr1^{fl/fl}*). To generate cardiac-

specific FXR1 knockout (cKO) mice, Cre recombinase was expressed from cardiomyocyte-specific α -MHC promoter.³⁶ Immunoblot analysis revealed no detectable FXR1 protein expression in LV of cKO mice (Figure 8C). The cKO mice appear indistinguishable from their WT littermates and have no overt signs of distress at 2 months. However, histological analysis of cKO hearts revealed enlarged ventricular lumens (Figure 8A). Transthoracic M-mode echocardiography at level of the papillary muscle confirmed that cKO hearts display a DCM phenotype with a significant increase in LV internal diameter and eccentric index (Figure 8B). Surprisingly, Cx43 and Cx45 protein and mRNA expression are not altered (Figure 8C, Supplemental Figure 9), while ZO-1 protein is significantly increased (Figure 8C). The increase in ZO-1 protein is consistent with the change seen in our other DCM mouse models (i.e., MLP- and LMOD2-KO, Supplemental Figures 4–5) and seems to be a common feature of DCM. Although ZO-1 protein is increased, its mRNA is significantly decreased in cKO mice and supports the role that FXR1 stabilizes ZO-1 mRNA (Supplemental Figure 7). The fact that FXR1 cKO hearts are dilated but there is no change in Cx43 protein expression as is commonly seen in other dilated cardiomyopathy samples (e.g., human and mouse models of DCM) is 1) consistent with our observation that up-regulation of FXR1 in DCM reduces Cx43 expression, and 2) strongly supports our hypothesis that FXR1 directly regulates Cx43 expression. Together, using cardiac-specific FXR1 KO mice we have demonstrated that FXR1 protein expression is involved in gap junction remodeling seen in DCM.

DISCUSSION

Dyregulation of the intercalated disc may contribute importantly to the phenotype of DCM and arrhythmia that is a major cause of morbidity and mortality. Understanding the precise mechanism by which gap junctions become abnormal may lead to new therapeutic targets for patients with heart failure due to DCM. Studies investigating the expression and localization of intercalated discs proteins in mouse models of DCM show several proteins are significantly altered including ZO-1 and Cx43 (for review³⁷). Changes in these proteins reduce cell-cell coupling and contribute to a more arrhythmogenic phenotype; the regulatory mechanism controlling the expression of these proteins is unknown. Since no direct links between gap junctional complex proteins and mRNA expression were reported prior to this investigation, it left open the possibility that post-transcriptional regulation is an important mechanism in cardiac disease progression. In fact, several studies have demonstrated that RNA binding proteins play a role in cardiac development and disease but how they do so is unknown (for review³⁸).

In this investigation, we discovered that the RNA binding protein FXR1 is an important mediator of gap junction remodeling associated with DCM. FXR1 plays multiple, functional roles by differentially regulating each of its targets by a unique mechanism; this regulation appears to depend on FXR1 expression levels. In left ventricles of human patients and mice with DCM, FXR1 protein expression is increased. This finding is consistent with data from gene profiling studies of human patients with DCM, revealing that FXR1 is significantly upregulated.³⁹ FXR1 localizes to the intercalated disc and directly interacts with the coding sequence of the major gap junction components: Cx43, ZO-1 and Cx45. FXR1 significantly alters Cx43 and ZO-1 protein expression. Functionally, upregulation of FXR1 in the heart

promotes redistribution of gap junctions contributing to an induced ventricular tachycardia in mice. Thus, we report FXR1-dependent mechanisms by which gap junctions are remodeled in DCM.

Cx43 is the major component of ventricular gap junctions and alterations in Cx43 expression are a consistent feature in DCM. In response to increased levels of FXR1, we show Cx43 protein expression and mRNA are reduced in isolated cardiomyocytes and intact hearts, as well as in human DCM samples. Accompanying the reduced Cx43 expression, a reduction and reorganization in gap junctions was observed. In addition to FXR1 contributing to Cx43 regulation in DCM, microRNAs are also critical regulators of gene expression in the heart. Cx43 mRNA has been shown to be the target of miR-1, miR-206 and miR-130a (for review⁴⁰). Interestingly, FXR1 interacts with the microRNA pathway via direct binding of Dicer and Argonaute 2.²⁰ Targeted deletion of Dicer in the heart leads to DCM, and an increase in Cx45, but not Cx43 protein expression.⁴¹ It is possible that changes in FXR1 levels alter the miRNA pathway, possibly increasing expression of microRNA's like miR-1, miR-206 and miR-130a, resulting in a decrease of Cx43 mRNA. Therefore, FXR1 directly represses Cx43 translation, but may be indirectly reducing its mRNA levels via the microRNA pathway.

ZO-1 directly interacts with Cx43 and upregulation of ZO-1 has been reported to correlate with downregulation of Cx43 protein and reduced gap junction plaque size.^{9–11} In human DCM, ZO-1 expression appears to be variable – an observation seen in our study and others.^{9–11} Intriguingly, a possible explanation for this reported variation is ZO-1 expression varies depending on levels of FXR1 expression. Specifically, in neonatal cardiomyocytes where expression levels of FXR1 can be controlled, we discovered that varying FXR1 expression affects ZO-1 expression; that is, low levels (~5 fold over endogenous) of FXR1 enhances ZO-1 protein expression, while high levels (~10 fold over endogenous) represses ZO-1 protein expression. Based on this finding, we predict that high variation between ZO-1 levels in human DCM samples that has been reported by many groups is due to variation in FXR1 expression.

Fragile × RNA-binding protein family members are known for their ability to regulate mRNA translation. Fragile × proteins also localize target mRNAs and control mRNA stability.^{23,42} Although ZO-1 protein is increased in mouse models of DCM (e.g., MLP-, LMOD2- and cardiac specific FXR1-KO mice) it does not appear to be translationally regulated by FXR1. Interestingly, while total ZO-1 mRNA levels are unaffected by elevated FXR1, ZO-1 mRNA stability is increased in isolated cardiomyocytes with elevated levels of FXR1. This finding that FXR1 regulates ZO-1 mRNA stability is further supported in cardiac-specific FXR1-KO mice (*fxr1^{fl/fl}* Myh6-Cre), which have reduced ZO-1 mRNA levels suggesting that loss of FXR1 leads to a loss of ZO-1 mRNA stability. An increase in mRNA stability was also seen for Cx45. Although we show FXR1 interacts with Cx45, it does not appear to directly regulate its translation. Therefore, the increase in stability of Cx45 and ZO-1 mRNA upon overexpression of FXR1 could be due to FXR1's role in stress granule formation. Stress granules are a type of cytoplasmic mRNA-protein aggregate complex that under cellular stress protects non-translating mRNA from degradation (for review⁴³). It is possible that FXR1 protects ZO-1 mRNA by translocating its transcripts into

stress granules. However, since loss of FXR1 results in increased ZO-1 protein it suggests other translational regulators are involved in regulating ZO-1 protein expression in DCM.

Studies have shown that upregulation of Cx45, particularly superimposed on down-regulation of Cx43, contributes to increased arrhythmias in the failing heart.^{34,44} Although no change was seen in levels of Cx45 protein (at the age studied) in the FXR1 overexpression mouse model it could still contribute to the arrhythmogenic phenotype since we found that increased levels of FXR1 in the heart significantly reduced Cx43 protein expression. This decrease in Cx43 would be expected to alter the Cx43:Cx45 ratio in connexons and channels, potentially having substantial effects on channel properties, resulting in arrhythmias. Conversely, non-uniform Cx43 gap junction distribution leads to the development of re-entrant circuits and clinically relevant arrhythmia in challenged hearts (e.g.,⁴⁵). Due to the inherent distribution of repolarization times throughout the myocardium that are often exacerbated in disease-states, atypical distribution of gap junctions may increase the likelihood that an isolated depolarization (often a premature ventricular contraction originating from a delay after depolarization) captures the myocardium in an uncontrollably propagating manner, as seen in programmed electrical stimulation of AAV-3xMycFXR1 injected mice (Figure 7A).

The FXR1 overexpression mouse model demonstrated increased vulnerability to ventricular arrhythmias. Interesting, no detectable abnormalities in cardiac function (via echocardiography) or structural abnormalities (via istaining for α -actinin and filamentous actin (data not shown)) were observed. Thus, our model may be useful for studying mechanisms leading to lethal arrhythmias in heart failure patients with elevated FXR1 levels. How FXR1 is regulated in disease is still not known. To date, there are no reports of FXR1 mutations associated with human disease (which is not surprising since FXR1 KO mice die shortly after birth).¹³ Alterations in FXR1 expression have not only been associated with human DCM (this study and³⁹) but have been associated with facioscapulohumeral muscular dystrophy and various cancers (i.e., lung, breast, ovarian, head and neck cancer).^{46,47} We previously reported that FXR1 interacts with its own transcript within the coding region resulting in repressed FXR1 translation.¹⁵ There are reports that miRNA pathways can regulate FXR1 protein expression.⁴⁸ Therefore, it is possible that FXR1 regulates its own translation in cardiomyopathy via direct interaction with its transcript or indirectly via the microRNA pathway. The precise mechanism by which FXR1 is regulated is the subject of ongoing investigations.

Clearly FXR1 may be a promising target for therapeutic strategies to improve gap junction function. Directly targeting RNA binding proteins for therapeutics for any disease is in early stages. For example, investigators have identified several compounds to block the RNA binding protein, Musashi-1 from interacting with RNA^{49,50}. Inhibition of Musashi-1's RNA binding ability has shown promising outcomes in preclinical studies for treating colon cancer. Future studies are necessary to examine whether inhibiting FXR1's function, expression or interaction with specific RNA can decrease the risk of arrhythmogenesis by preventing gap junction remodeling.

In summary, our findings on FXR1 and its novel target mRNAs provides a compelling mechanism for gap junction remodeling associated with dilated cardiomyopathy. To our knowledge, the results presented in this study are the first to show a connection between FXR1 levels, dilated cardiomyopathy, arrhythmogenesis and regulation of expression of major gap junction proteins Cx43, Cx45 and ZO-1. Taking together, FXR1 is a multi-functional protein involved not only cardiac development but also cardiac disease.

Supplementary Material

Refer to Web version on PubMed Central for supplementary material.

Acknowledgments

We thank Dr. Allen Samarel from Loyola University Chicago for human tissue samples; Maribeth Stansifer for assistance with electrophysiology studies; Rachel Mayfield for generating cultures; Dr. Bhavani Siddegowda for polysome protocol and Stephen Yao for technical help with this assay; Jose Valdez for help with cell patterning; Dr. Samantha Whitman for initiating the project; Dr. Nancy Sweitzer for insightful editing; and Drs. Nancy Sweitzer, Christopher Pappas, Steven Goldman, Janis Burt and Jose Ek Vitorin for thoughtful discussions.

Sources of Funding

This work was supported by American Heart Association (16POST27260153) and Sarver Heart Center (J.G. Murray/Anthony and Mary Zoia Awards) to MC; NIH Fellowship (1F31HL117520) and Achievement Rewards for College Students to SMN; Sarver Heart Center to EBJ; American Heart Association (0930170N) to DCZ; NIH grant (DP2OD007161) to PKW; and NIH grants (R01HL108625 and R01HL123078) to CCG.

References

- Spezzacatene A, Sinagra G, Merlo M, Barbati G, Graw SL, Brun F, Slavov D, Di Lenarda A, Salcedo EE, Towbin JA, Saffitz JE, Marcus FI, Zareba W, Taylor MRG, Mestroni L. Familial Cardiomyopathy Registry. Arrhythmogenic Phenotype in Dilated Cardiomyopathy: Natural History and Predictors of Life-Threatening Arrhythmias. *J Am Heart Assoc.* 2015; 4:e002149.doi: 10.1161/JAHA.115.002149 [PubMed: 26475296]
- Ferreira-Cornwell MC, Luo Y, Narula N, Lenox JM, Lieberman M, Radice GL. Remodeling the intercalated disc leads to cardiomyopathy in mice misexpressing cadherins in the heart. *J Cell Sci.* 2002; 115:1623–1634. [PubMed: 11950881]
- Lambiase PD, Tinker A. Connexins in the heart. *Cell Tissue Res.* 2015; 360:675–684. DOI: 10.1007/s00441-014-2020-8 [PubMed: 25358402]
- Kostin S, Rieger M, Dammer S, Hein S, Richter M, Klövekorn W-P, Bauer EP, Schaper J. Gap junction remodeling and altered connexin 43 expression in the failing human heart. *Mol Cell Biochem.* 2003; 242:135–144. [PubMed: 12619876]
- Danik SB, Liu F, Zhang J, Suk HJ, Morley GE, Fishman GI, Gutstein DE. Modulation of cardiac gap junction expression and arrhythmic susceptibility. *Circ Res.* 2004; 95:1035–1041. DOI: 10.1161/01.RES.0000148664.33695.2a [PubMed: 15499029]
- Yao J-A, Gutstein DE, Liu F, Fishman GI, Wit AL. Cell coupling between ventricular myocyte pairs from connexin43-deficient murine hearts. *Circ Res.* 2003; 93:736–743. DOI: 10.1161/01.RES.0000095977.66660.86 [PubMed: 14500334]
- Kurtenbach S, Kurtenbach S, Zoidl G. Gap junction modulation and its implications for heart function. *Front Physiol.* 2014; 5:82.doi: 10.3389/fphys.2014.00082 [PubMed: 24578694]
- Palatinus JA, O'Quinn MP, Barker RJ, Harris BS, Jourdan J, Gourdie RG. ZO-1 determines adherens and gap junction localization at intercalated disks. *Am J Physiol Heart Circ Physiol.* 2011; 300:H583–594. DOI: 10.1152/ajpheart.00999.2010 [PubMed: 21131473]

9. Toyofuku T, Yabuki M, Otsu K, Kuzuya T, Hori M, Tada M. Direct association of the gap junction protein connexin-43 with ZO-1 in cardiac myocytes. *J Biol Chem.* 1998; 273:12725–12731. [PubMed: 9582296]
10. Hunter AW, Barker RJ, Zhu C, Gourdie RG. Zonula occludens-1 alters connexin43 gap junction size and organization by influencing channel accretion. *Mol Biol Cell.* 2005; 16:5686–5698. DOI: 10.1091/mbc.E05-08-0737 [PubMed: 16195341]
11. Bruce AF, Rothery S, Dupont E, Severs NJ. Gap junction remodelling in human heart failure is associated with increased interaction of connexin43 with ZO-1. *Cardiovasc Res.* 2008; 77:757–765. DOI: 10.1093/cvr/cvm083 [PubMed: 18056766]
12. Lukong KE, Chang K-W, Khandjian EW, Richard S. RNA-binding proteins in human genetic disease. *Trends Genet.* 2008; 24:416–425. DOI: 10.1016/j.tig.2008.05.004 [PubMed: 18597886]
13. Mientjes EJ, Willemsen R, Kirkpatrick LL, Nieuwenhuizen IM, Hoogeveen-Westerveld M, Verweij M, Reis S, Barboni B, Hoogeveen AT, Oostra BA, Nelson DL. Fxr1 knockout mice show a striated muscle phenotype: implications for Fxr1p function in vivo. *Hum Mol Genet.* 2004; 13:1291–1302. DOI: 10.0193/hmg/ddh150 [PubMed: 15128702]
14. van't Padje S, Chaudhry B, Severijnen LA, van der Linde HC, Mientjes EJ, Oostra BA, Willemsen R. Reduction in fragile × related 1 protein causes cardiomyopathy and muscular dystrophy in zebrafish. *J Exp Biol.* 2009; 212:2564–2570. DOI: 10.1242/jeb.032532 [PubMed: 19648401]
15. Whitman SA, Cover C, Yu L, Nelson DL, Zarnescu DC, Gregorio CC. Desmoplakin and Talin2 Are Novel mRNA Targets of Fragile X-Related Protein-1 in Cardiac Muscle. *Circ Res.* 2011; 109:262–271. DOI: 10.1161/CIRCRESAHA.111.244244 [PubMed: 21659647]
16. Zhang Y, O'Connor JP, Siomi MC, Srinivasan S, Dutra A, Nussbaum RL, Dreyfuss G. The fragile × mental retardation syndrome protein interacts with novel homologs FXR1 and FXR2. *EMBO J.* 1995; 14:5358–5366. [PubMed: 7489725]
17. Darnell JC, Jensen KB, Jin P, Brown V, Warren ST, Darnell RB. Fragile × mental retardation protein targets G quartet mRNAs important for neuronal function. *Cell.* 2001; 107:489–499. [PubMed: 11719189]
18. Ascano M, Mukherjee N, Bandaru P, Miller JB, Nusbaum JD, Corcoran DL, Langlois C, Munschauer M, Dewell S, Hafner M, Williams Z, Ohler U, Tuschl T. FMRP targets distinct mRNA sequence elements to regulate protein expression. *Nature.* 2012; 492:382–386. DOI: 10.1038/nature11737 [PubMed: 23235829]
19. Bakker CE, de Diego Otero Y, Bontekoe C, Raghoe P, Luteijn T, Hoogeveen AT, Oostra BA, Willemsen R. Immunocytochemical and Biochemical Characterization of FMRP, FXR1P, and FXR2P in the Mouse. *Exp Cell Res.* 2000; 258:162–170. DOI: 10.1006/excr.2000.4932 [PubMed: 10912798]
20. Vasudevan S, Steitz JA. AU-Rich-Element-Mediated Upregulation of Translation by FXR1 and Argonaute 2. *Cell.* 2007; 128:1105–1118. DOI: 10.1016/j.cell.2007.01.038 [PubMed: 17382880]
21. Khera TK, Dick AD, Nicholson LB. Fragile X-related protein FXR1 controls post-transcriptional suppression of lipopolysaccharide-induced tumour necrosis factor- α production by transforming growth factor- β 1. *FEBS J.* 2010; 277:2754–2765. DOI: 10.1111/j.1742-4658.2010.07692.x [PubMed: 20491901]
22. Ye W, Qin F, Zhang J, Luo R, Chen H-F. Atomistic mechanism of microRNA translation upregulation via molecular dynamics simulations. *PLoS ONE.* 2012; 7:e43788.doi: 10.1371/journal.pone.0043788 [PubMed: 22952765]
23. Davidovic L, Durand N, Khalfallah O, Tabet R, Barbry P, Mari B, Sacconi S, Moine H, Bardoni B. A novel role for the RNA-binding protein FXR1P in myoblasts cell-cycle progression by modulating p21/Cdkn1a/Cip1/Waf1 mRNA stability. *PLoS Genet.* 2013; 9:e1003367.doi: 10.1371/journal.pgen.1003367 [PubMed: 23555284]
24. Chu M, Koshman Y, Iyengar R, Kim T, Russell B, Samarel AM. Contractile Activity Regulates Inducible Nitric Oxide Synthase Expression and NO iProduction in Cardiomyocytes via a FAK-Dependent Signaling Pathway. *J Sig Transd.* 2012; 2012:1–11. DOI: 10.1155/2012/473410
25. Manso AM, Li R, Monkley SJ, Cruz NM, Ong S, Lao DH, Koshman YE, Gu Y, Peterson KL, Chen J, Abel ED, Samarel AM, Critchley DR, Ross RS. Talin1 has unique expression versus talin

- 2 in the heart and modifies the hypertrophic response to pressure overload. *J Biol Chem.* 2013; 288:4252–4264. DOI: 10.1074/jbc.M112.427484 [PubMed: 23266827]
26. Koczor CA, Lee EK, Torres RA, Boyd A, Vega JD, Uppal K, Yuan F, Fields EJ, Samarel AM, Lewis W. Detection of differentially methylated gene promoters in failing and nonfailing human left ventricle myocardium using computation analysis. *Physiol Genomics.* 2013; 45:597–605. DOI: 10.1152/physiolgenomics.00013.2013 [PubMed: 23695888]
 27. Koshman YE, Patel N, Chu M, Iyengar R, Kim T, Ersahin C, Lewis W, Heroux A, Samarel AM. Regulation of Connective Tissue Growth Factor Gene Expression and Fibrosis in Human Heart Failure. *J Card Fail.* 2013; 19:283–294. DOI: 10.1016/j.cardfail.2013.01.013 [PubMed: 23582094]
 28. Pappas CT, Mayfield RM, Henderson C, Jamilpour N, Cover C, Hernandez Z, Hutchinson KR, Chu M, Nam K-H, Valdez JM, Wong PK, Granzier HL, Gregorio CC. Knockout of Lmod2 results in shorter thin filaments followed by dilated cardiomyopathy and juvenile lethality. *Proc Natl Acad Sci USA.* 2015; 112:13573–13578. DOI: 10.1073/pnas.1508273112 [PubMed: 26487682]
 29. Arber S, Hunter JJ, Ross J, Hongo M, Sansig G, Borg J, Perriard JC, Chien KR, Caroni P. MLP-deficient mice exhibit a disruption of cardiac cytoarchitectural organization, dilated cardiomyopathy, and heart failure. *Cell.* 1997; 88:393–403. [PubMed: 9039266]
 30. Mazroui R, Huot M-E, Tremblay S, Filion C, Labelle Y, Khandjian EW. Trapping of messenger RNA by Fragile × Mental Retardation protein into cytoplasmic granules induces translation repression. *Hum Mol Genet.* 2002; 11:3007–3017. [PubMed: 12417522]
 31. Perriard J-C, Hirschy A, Ehler E. Dilated cardiomyopathy: a disease of the intercalated disc? *Trends Cardiovasc Med.* 2003; 13:30–38.
 32. Kikin O, D'Antonio L, Bagga PS. QGRS Mapper: a web-based server for predicting G-quadruplexes in nucleotide sequences. *Nucleic Acids Res.* 2006; 34:W676–82. DOI: 10.1093/nar/gkl253 [PubMed: 16845096]
 33. Li J, Patel VV, Kostetskii I, Xiong Y, Chu AF, Jacobson JT, Yu C, Morley GE, Molkentin JD, Radice GL. Cardiac-specific loss of N-cadherin leads to alteration in connexins with conduction slowing and arrhythmogenesis. *Circ Res.* 2005; 97:474–481. doi: 10.1161.01.RES.0000181132.11393.18. [PubMed: 16100040]
 34. Yamada KA, Rogers JG, Sundset R, Steinberg TH, Saffitz JE. Up-regulation of connexin45 in heart failure. *J Cardiovasc Electr.* 2003; 14:1205–1212.
 35. Ehler E, Horowitz R, Zuppinger C, Price RL, Perriard E, Leu M, Caroni P, Sussman M, Eppenberger HM, Perriard JC. Alterations at the intercalated disk associated with the absence of muscle LIM protein. *J Cell Biol.* 2001; 153:763–772. [PubMed: 11352937]
 36. Agah R, Frenkel PA, French BA, Michael LH, Overbeek PA, Schneider MD. Gene recombination in postmitotic cells. Targeted expression of Cre recombinase provokes cardiac-restricted, site-specific rearrangement in adult ventricular muscle in vivo. *J Clin Invest.* 1997; 100:169–179. DOI: 10.1172/JCI119509 [PubMed: 9202069]
 37. Pluess M, Daeubler G, Remedios dos CG, Ehler E. Adaptations of cytoarchitecture in human dilated cardiomyopathy. *Biophys Rev.* 2015; 7:25–32. DOI: 10.1007/s12551-014-0146-2
 38. Zarnescu DC, Gregorio CC. Fragile hearts: New insights into translational control in cardiac muscle. *Trends Cardiovasc Med.* 2013; 23:275–281. DOI: 10.1016/j.tcm.2013.03.003
 39. Yung CK, Halperin VL, Tomaselli GF, Winslow RL. Gene expression profiles in end-stage human idiopathic dilated cardiomyopathy: altered expression of apoptotic and cytoskeletal genes. *Genom.* 2004; 83:281–297.
 40. Ono K, Kuwabara Y, Han J. MicroRNAs and cardiovascular diseases. *FEBS J.* 2011; 278:1619–1633. DOI: 10.1111/j.1742-4658.2011.08090.x [PubMed: 21395978]
 41. Chen J-F, Murchison EP, Tang R, Callis TE, Tatsuguchi M, Deng Z, Rojas M, Hammond SM, Schneider MD, Selzman CH, Meissner G, Patterson C, Hannon GJ, Wang D-Z. Targeted deletion of Dicer in the heart leads to dilated cardiomyopathy and heart failure. *Proc Natl Acad Sci USA.* 2008; 105:2111–2116. DOI: 10.1073/pnas.0710228105 [PubMed: 18256189]
 42. Antar LN, Dichtenberg JB, Plociniak M, Afroz R, Bassell GJ. Localization of FMRP-associated mRNA granules and requirement of microtubules for activity-dependent trafficking in hippocampal neurons. *Genes Brain Behav.* 2005; 4:350–359. DOI: 10.1111/j.1601-183X.2005.00128.x [PubMed: 16098134]

43. Buchan JR, Parker R. Eukaryotic Stress Granules: The Ins and Outs of Translation. *Mol Cell*. 2009; 36:932–941. DOI: 10.1016/j.molcel.2009.11.020 [PubMed: 20064460]
44. Betsuyaku T, Nnebe NS, Sundset R, Patibandla S, Krueger CM, Yamada KA. Overexpression of cardiac connexin45 increases susceptibility to ventricular tachyarrhythmias in vivo. *Am J Physiol Heart Circ Physiol*. 2006; 290:H163–171. DOI: 10.1152/ajpheart.01308.2004 [PubMed: 16126808]
45. Peters NS, Coromilas J, Severs NJ, Wit AL. Disturbed connexin43 gap junction distribution correlates with the location of reentrant circuits in the epicardial border zone of healing canine infarcts that cause ventricular tachycardia. *Circ*. 1997; 95:988–996.
46. Davidovic L, Sacconi S, Bechara EG, Delplace S, Allegra M, Desnuelle C, Bardoni B. Alteration of expression of muscle specific isoforms of the fragile × related protein 1 (FXR1P) in facioscapulohumeral muscular dystrophy patients. *J Med Genet*. 2008; 45:679–685. DOI: 10.1136/jmg.2008.060541 [PubMed: 18628314]
47. Qian J, Hassanein M, Hoeksema MD, Harris BK, Zou Y, Chen H, Lu P, Eisenberg R, Wang J, Espinosa A, Ji X, Harris FT, Rahman SMJ, Massion PP. The RNA binding protein FXR1 is a new driver in the 3q26-29 amplicon and predicts poor prognosis in human cancers. *Proc Natl Acad Sci USA*. 2015; 112:3469–3474. DOI: 10.1073/pnas.1421975112 [PubMed: 25733852]
48. Cheever A, Blackwell E, Ceman S. Fragile × protein family member FXR1P is regulated by microRNAs. *RNA*. 2010; 16:1530–1539. DOI: 10.1261/rna.2022210 [PubMed: 20519410]
49. Lan L, Appelman C, Smith AR, Yu J, Larsen S, Marquez RT, Liu H, Wu X, Gao P, Roy A, Anbanandam A, Gowthaman R, Karanicolas J, De Guzman RN, Rogers S, Aubé J, Ji M, Cohen RS, Neufeld KL, Xu L. Natural product (–)-gossypol inhibits colon cancer cell growth by targeting RNA-binding protein Musashi-1. *Mol Oncol*. 2015; 9:1406–1420. DOI: 10.1016/j.molonc.2015.03.014 [PubMed: 25933687]
50. Clingman CC, Deveau LM, Hay SA, Genga RM, Shandilya SMD, Massi F, Ryder SP. Allosteric inhibition of a stem cell RNA-binding protein by an intermediary metabolite. *Elife*. 2014; 3:693.doi: 10.7554/eLife.02848

CLINICAL PERSPECTIVE

What is new?

- FXR1 expression is significantly increased in human and mouse dilated cardiomyopathy (DCM).
- Upregulation of FXR1 in the heart alters localization and distribution of gap junctions subsequently leading to ventricular tachycardia in mice.
- FXR1 associates with intercalated discs and directly interacts with Cx43, Cx45 and ZO-1 mRNA to regulate their expression in cardiomyocytes.
- Loss of FXR1 in the heart leads to DCM with no observable change in Cx43 expression, as is seen in hearts from other DCM models.

What are the clinical implications?

- The present study identifies a novel mechanism whereby the RNA-binding protein FXR1 directly regulates gap junction remodeling, leading to DCM.
- FXR1 is a promising target for therapeutic strategies to improve gap junction function in DCM.

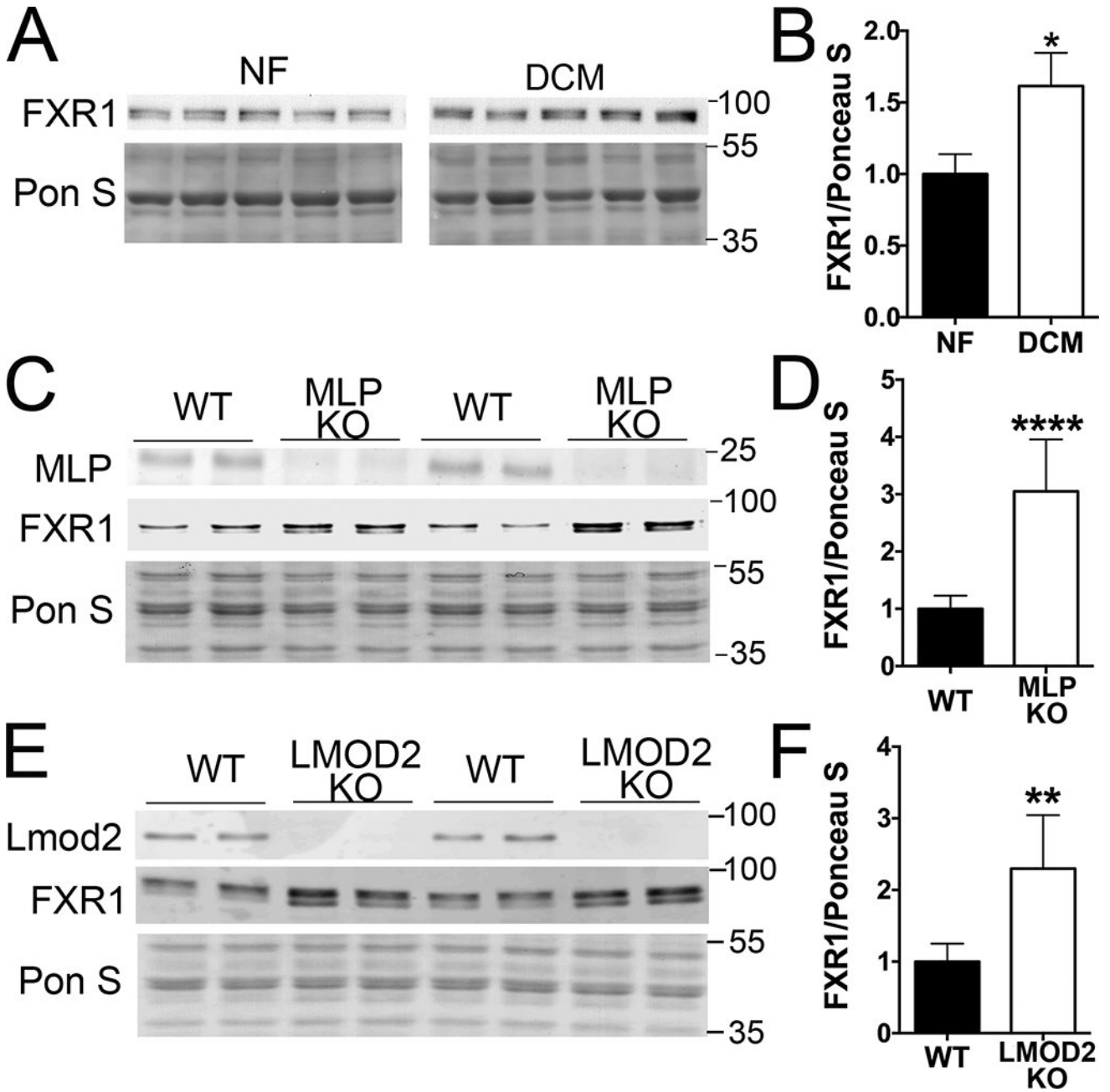


Figure 1. FXR1 is upregulated in human DCM and mouse models of DCM

(A,C,E) Representative immunoblots of human DCM, MLP and LMOD2 KO left ventricle lysates probed for FXR1, plus Ponceau S staining (for actin) of the blot used for normalization. (B,D,F) FXR1 is significantly elevated in all DCM models: human DCM (1.61±0.231 fold increase, n=8) normalized with non-failing (NF) samples (n=9), and MLP KO (3.05±0.343 fold increase, n=4) and LMOD2 KO (2.29±0.335 fold increase, n=4) mice normalized with respective WT samples (n=4). Student's t-test was used to calculate statistical significance: p values *p<0.05, ** p<0.01 and **** p<0.0001.

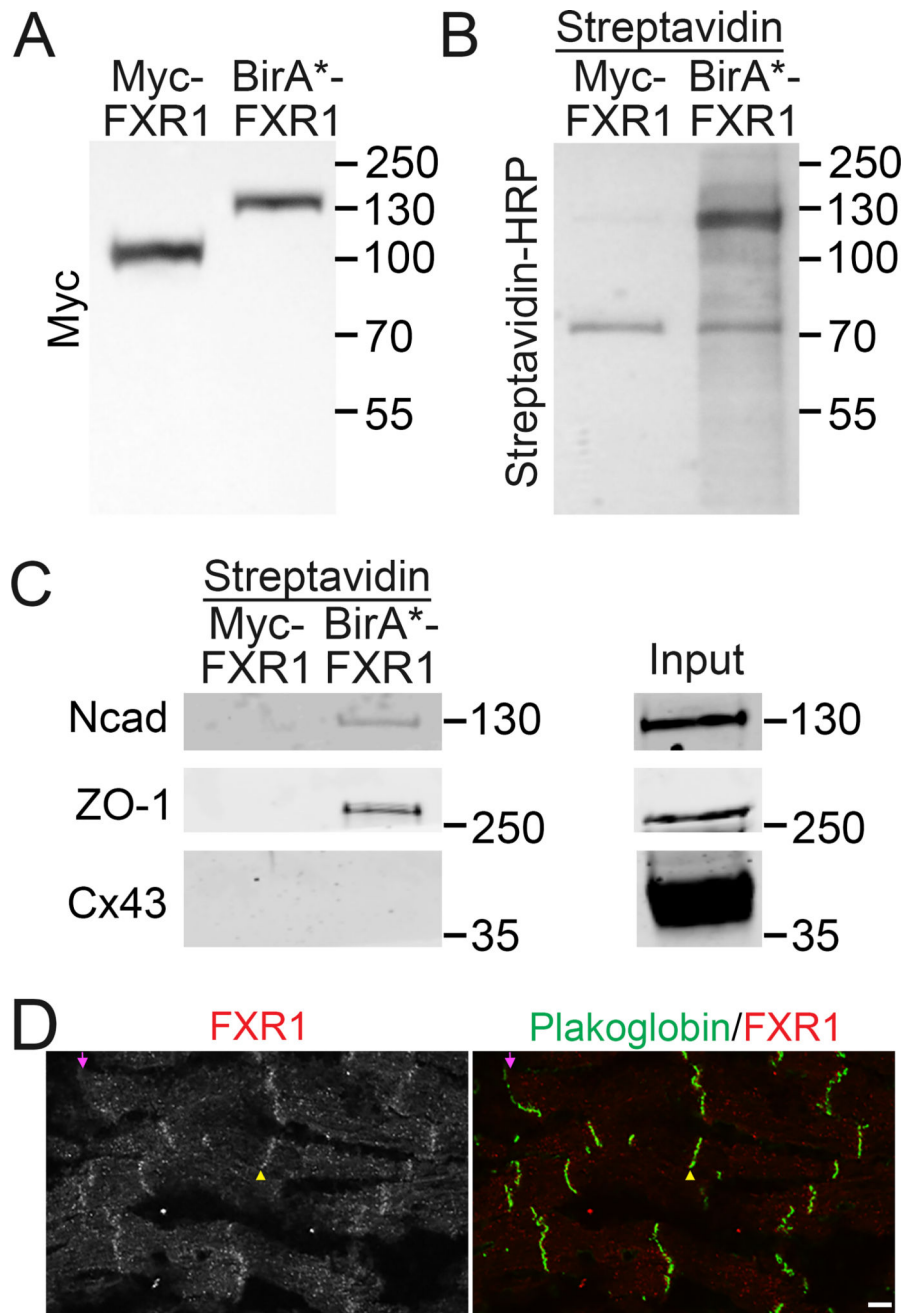


Figure 2. FXR1 associates with the intercalated discs

Neonatal rat cardiomyocytes were transduced with 3xMyc-FXR1 (Myc-FXR1) as a control or MycBirA*-FXR1 (BirA*-FXR1) adenovirus. **(A)** Representative immunoblots probed with an anti-Myc antibody demonstrating expression of exogenous 3xMyc-FXR1 or MycBirA*-FXR1. **(B)** Biotinylated proteins detected with HRP-conjugated streptavidin after SDS-PAGE separation of MycBirA*-FXR1 treated and 3xMyc-FXR1 control cells. **(C)** Biotinylated proteins from Bio-ID pull down were resolved on a SDS-polyacrylamide gel and subjected to immunoblotting with antibodies to the intercalated disc proteins N-cadherin (Ncad), ZO-1 and Cx43. Ncad and ZO-1 but not Cx43 were enriched in cells expressing

MycBirA*-FXR1. **(D)** Representative confocal images show that while FXR1 (red) is localized in numerous intracellular locations as demonstrated previously (e.g.,^{13,19}), it is also specifically enriched in close proximity to intercalated discs as marked by anti-plakoglobin antibodies (green). Yellow arrowhead marks FXR1 at the intercalated disc; magenta arrowhead marks is intercalated disc without detectable FXR1. Scale bar = 10 μ m.

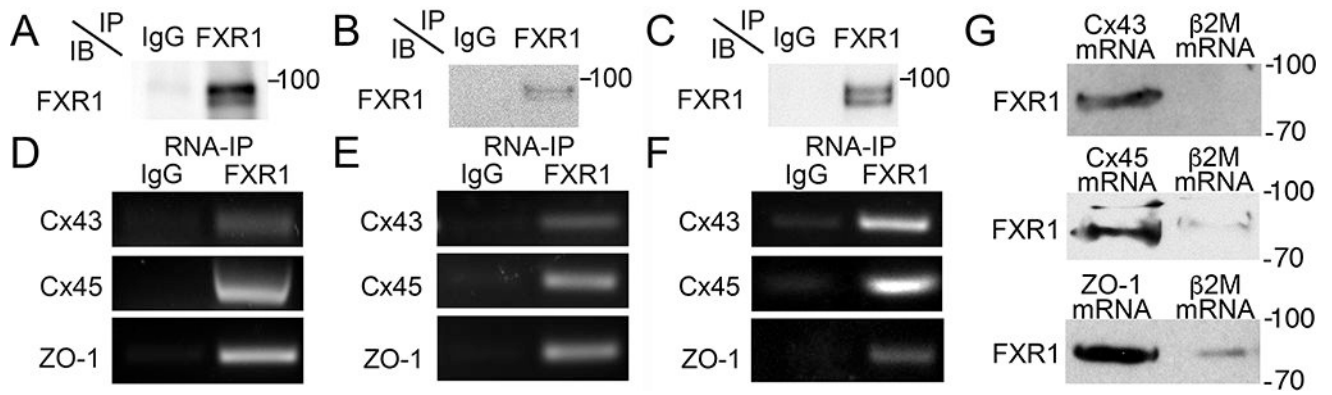


Figure 3. FXR1 directly interacts with Cx43, Cx45 and ZO-1 mRNAs

Endogenous FXR1 protein was immunoprecipitated (IP) from either human left ventricle (A,D), mouse left ventricle (B,E) or rat cardiomyocytes (C,F) using anti-FXR1 antibodies or IgG as a control. (A,B,C) Proteins from precipitated fractions were resolved on a SDS-polyacrylamide gel and subjected to immunoblotting (IB) with anti-FXR1 antibodies. FXR1 was detected in the FXR1-bound fraction but not in the IgG-bound fraction. (D,E,F) RNA isolated from the FXR1 RNA-IP was subjected to RT-PCR analysis using Cx43, Cx45 and ZO-1 primers. All three targets were detected in the FXR1-bound fraction but not in the IgG-bound fraction. (G) Biotin labeled β 2M (negative control), Cx43, Cx45 and ZO-1 mRNAs were incubated with recombinant FXR1 protein. The complex was resolved on a SDS-polyacrylamide gel and subjected to immunoblotting with anti-FXR1 antibodies. FXR1 bound to Cx43, Cx45 and ZO-1 mRNA but not β 2M mRNA.

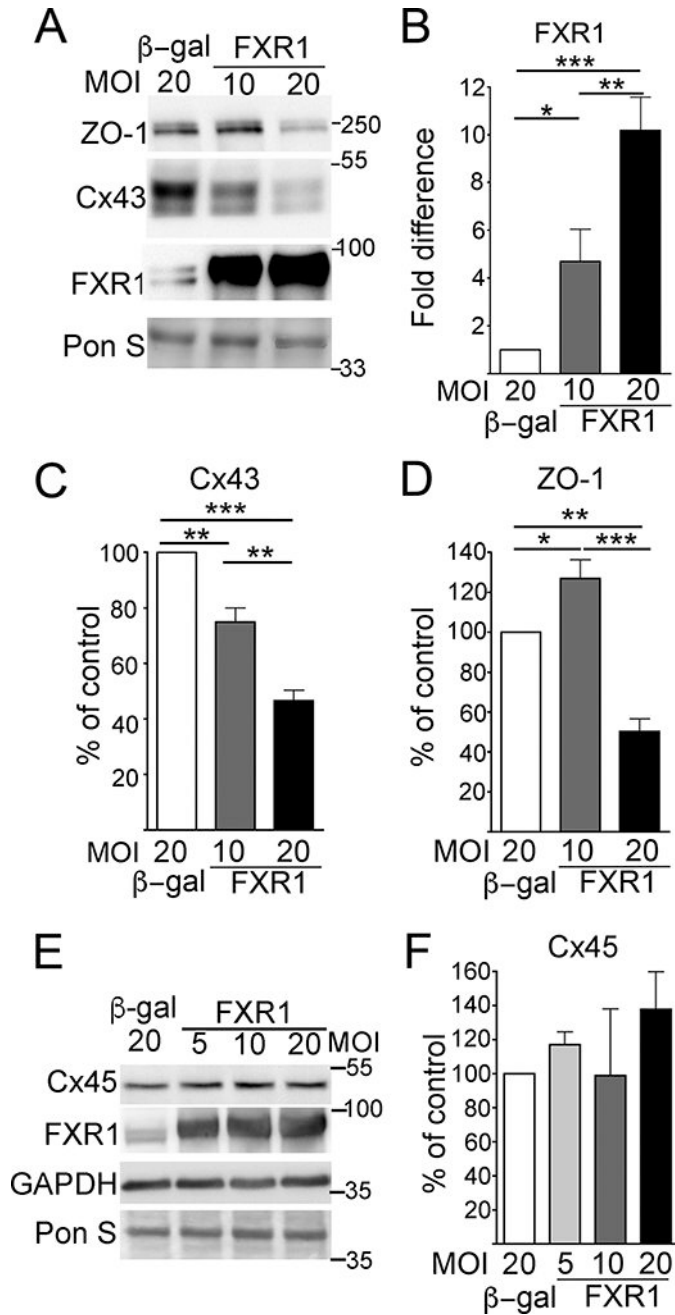


Figure 4. Overexpression of FXR1 reduces Cx43 and ZO-1 protein expression in rat cardiomyocytes

Cells were transduced with FXR1 or β-galactosidase (β-gal) adenovirus. (A) Representative immunoblots probed with antibodies against FXR1, Cx43 and ZO-1 plus Ponceau S staining (for actin) of the blot used for normalization. (B) FXR1 protein expression was expressed as fold increase compared with β-gal control. (C) Cx43 protein is reduced. Note the anti-Cx43 antibody recognizes different phosphorylation states of Cx43 (shown as multiple bands); for comparison between samples the total amount of Cx43 was quantified. (D) ZO-1 protein is increased at low levels of FXR1 overexpression and reduced at high levels of FXR1

overexpression compared with β -gal control. **(E)** Representative immunoblots probed for FXR1, Cx45, GAPDH and Ponceau S staining (for actin) of blot. **(F)** Cx45 levels are not significantly changed. Data are mean \pm SEM of at least four independent experiments. One-way ANOVA was used to calculate statistical significance: p values *p<0.05, ** p<0.01 and *** p<0.001.

Author Manuscript

Author Manuscript

Author Manuscript

Author Manuscript

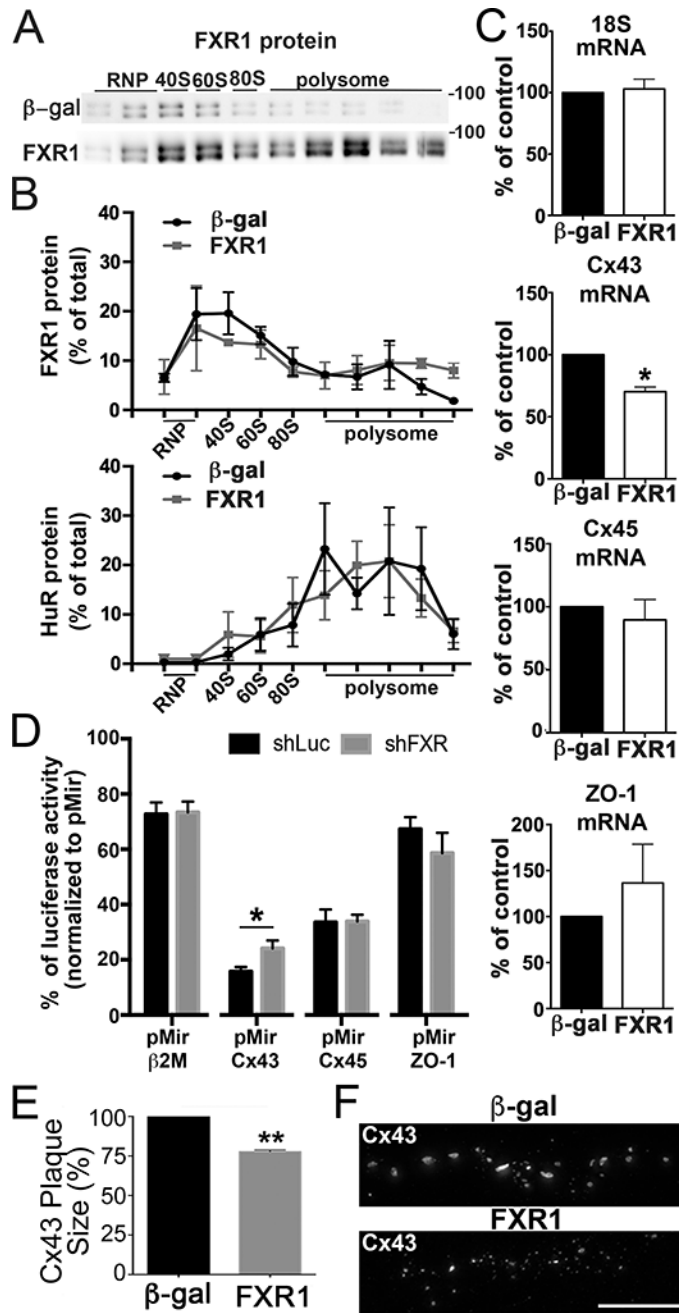


Figure 5. FXR1 is involved in translational regulation of Cx43 and ZO-1 mRNA
 Neonatal cardiomyocytes were transduced with Adv-FXR1 (10 MOI) or Adv β-galactosidase (β-gal, 10 MOI) for 72h and ribosomes from equivalent amounts of total RNA were fractionated (n=3). (A) FXR1 protein expression in different fractions from polysome profile reveals that FXR1 associates with both the RNP and polysome fractions. (B) Distribution of FXR1 and HuR protein levels (reported as percent FXR1 or HuR protein in each fraction divided by total FXR1 or HuR protein) in the polysome profile. A slight increase in FXR1 protein associated with the heavy polysome fraction is seen while no change is seen in HuR protein. (C) Percent of total Cx43 mRNA level (70.29% of control) is

reduced in the polysome fraction in FXR1 overexpression cells but no change is seen for 18S, Cx45 and ZO-1 mRNA. Student T-test was used to calculate statistical significance (n=3). **(D)** Luciferase activity is significantly reduced for pMirCx43 in cells expressing FXR1 (65.21% of shLuc compared to shFXR1). No change was seen for pMirZO-1 or pMirCx45 or the negative control pMir β 2M in cells expressing FXR1 (shLuc) compared to control (shFXR). pMir vector alone serves as control that is not translationally repressed by FXR1. Student's T-test analysis was used to calculate statistical significance for each pMir construct: p values * p<0.05. **(E)** Graph of Cx43 plaque sizes expressed as the percentage of β -gal control (average 22.29 \pm 0.605% smaller in FXR1 vs. β -gal). Data are means \pm SEM (n=3, average of 10 cells from three independent cultures). Student's T-test was used to calculate statistical significance: p value ** p<0.01. **(F)** Representative set of deconvolution images showing a decrease in Cx43 plaque size in cells overexpressing FXR1. Scale bar = 10 μ m.

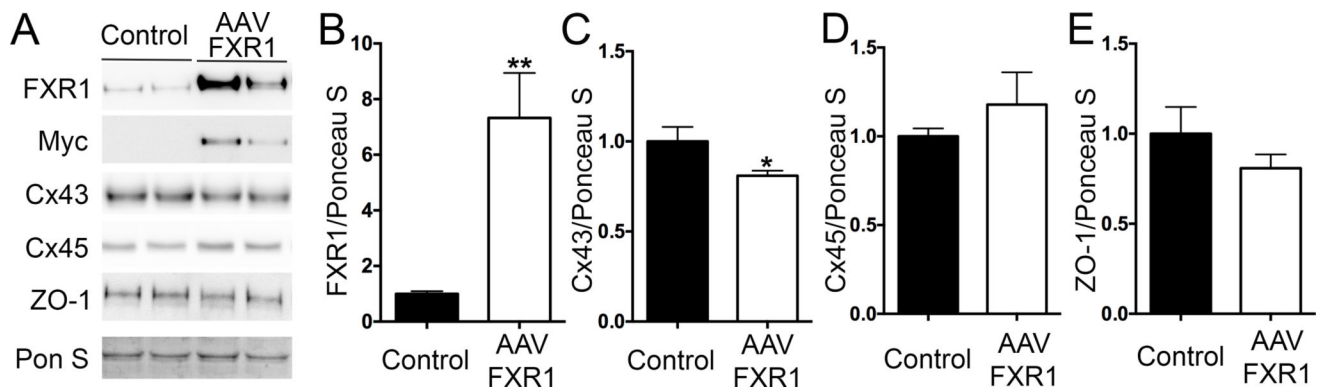


Figure 6. Overexpression of FXR1 in mouse heart reduces Cx43 protein expression

AAV-3xMyc-FXR1 was injected into D4 C57BL/6 mice and at D56 collected. (A) Representative immunoblots of control and AAV-3xMyc-FXR1 injected mice. Left ventricle lysates probed for FXR1, Myc, Cx43, Cx45 and ZO-1 plus Ponceau S staining (for actin) of the blot used for normalization. (B) FXR1 protein expression levels in AAV-3xMyc-FXR1 injected mice were significantly increased ($n=5$; 7.33 ± 1.62 , $p, 0.01$) compared with control ($n=4$). In AAV-3xMyc-FXR1 injected mice, (C) Cx43 protein expression is significantly reduced (0.809 ± 0.028 , $p < 0.05$) compared with control. (D) Cx45 and (E) ZO-1 protein levels are both unchanged. Students T-test was used to calculate statistical significance: p values * $p < 0.05$ and ** $p < 0.01$.

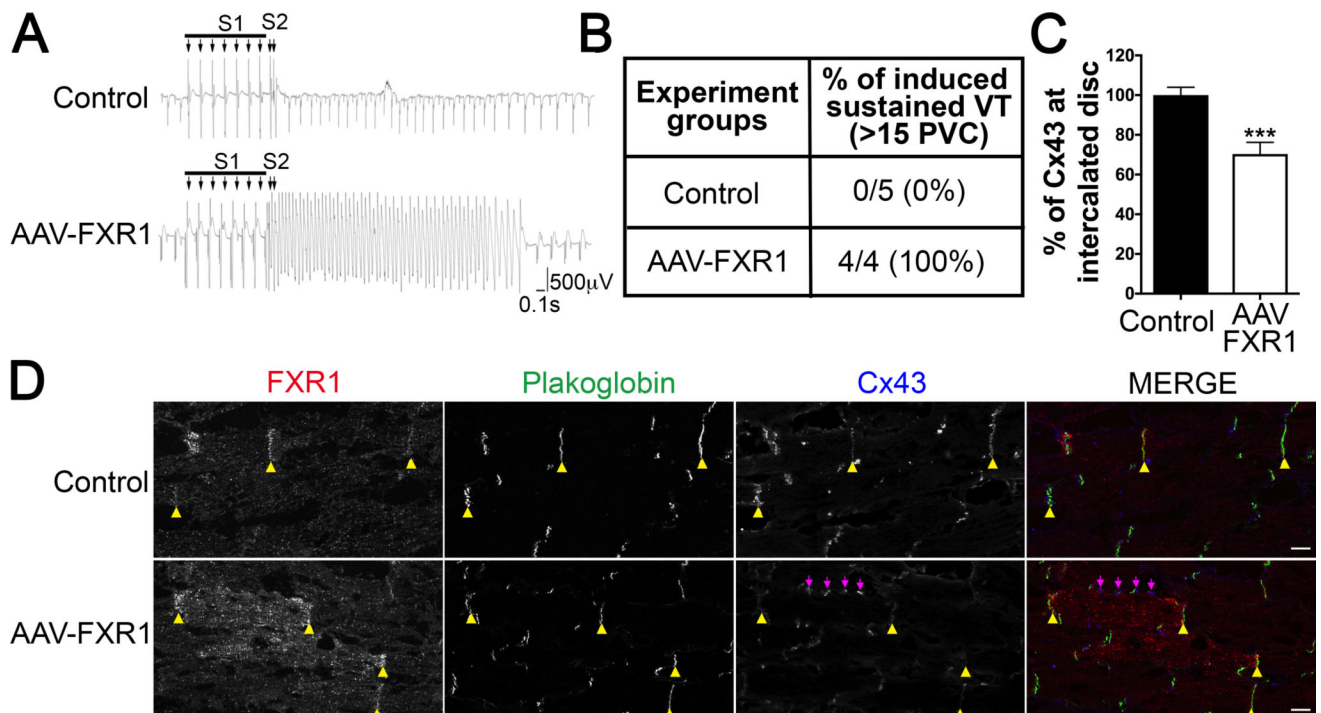


Figure 7. Overexpression of FXR1 in mice results in redistribution of gap junctions and promotes sustained ventricular tachycardia

AAV-3xMyc-FXR1 was injected into day 4 B56/BL mice. Between 2–3 months of age, electrophysiology studies were performed. **(A)** Examples of normal or ventricular tachycardia in control mice and in AAV-3xMyc-FXR1 injected mice. In AAV-3xMyc-FXR1 injected mice, a monomorphic sustained ventricular tachycardia ensues for approximately 4.3 seconds at a rate of approximately 960 beats/minute. Spontaneous recapture of the heart by the intrinsic conduction system terminates the sustained ventricular tachycardia, which is not seen in the control mice. **(B)** AAV-3xMyc-FXR1 injected mice have a significant ($n=4$, $p<0.05$) incidence of sustained ventricular tachycardia, defined as greater than fifteen consecutive premature ventricular contractions, compared to control ($n=5$). An unpaired T-test was used to calculate statistical significance. **(C)** The percent of Cx43 fluorescence intensity at the intercalated disc (ICD; as marked by plakoglobin). There is a significant reduction in Cx43 at the ICD in AAV-3xMyc-FXR1 injected compared to control mice ($n=20$, $70.32\pm 5.91\%$, $p<0.001$) versus cells with control levels of FXR1 ($n=20$, $100\pm 3.98\%$). Students T-test was used to calculate statistical significance: p value *** $p<0.001$. **(D)** Representative confocal images showing overexpression of FXR1 (red) in AAV-3xMyc-FXR1 injected mice results in redistribution of Cx43 (blue) from the intercalated disc (marked by yellow arrowheads) to along the lateral membrane (marked by magenta arrows). Plakoglobin (green) marks the intercalated disc. Scale bar = 10 μ m.

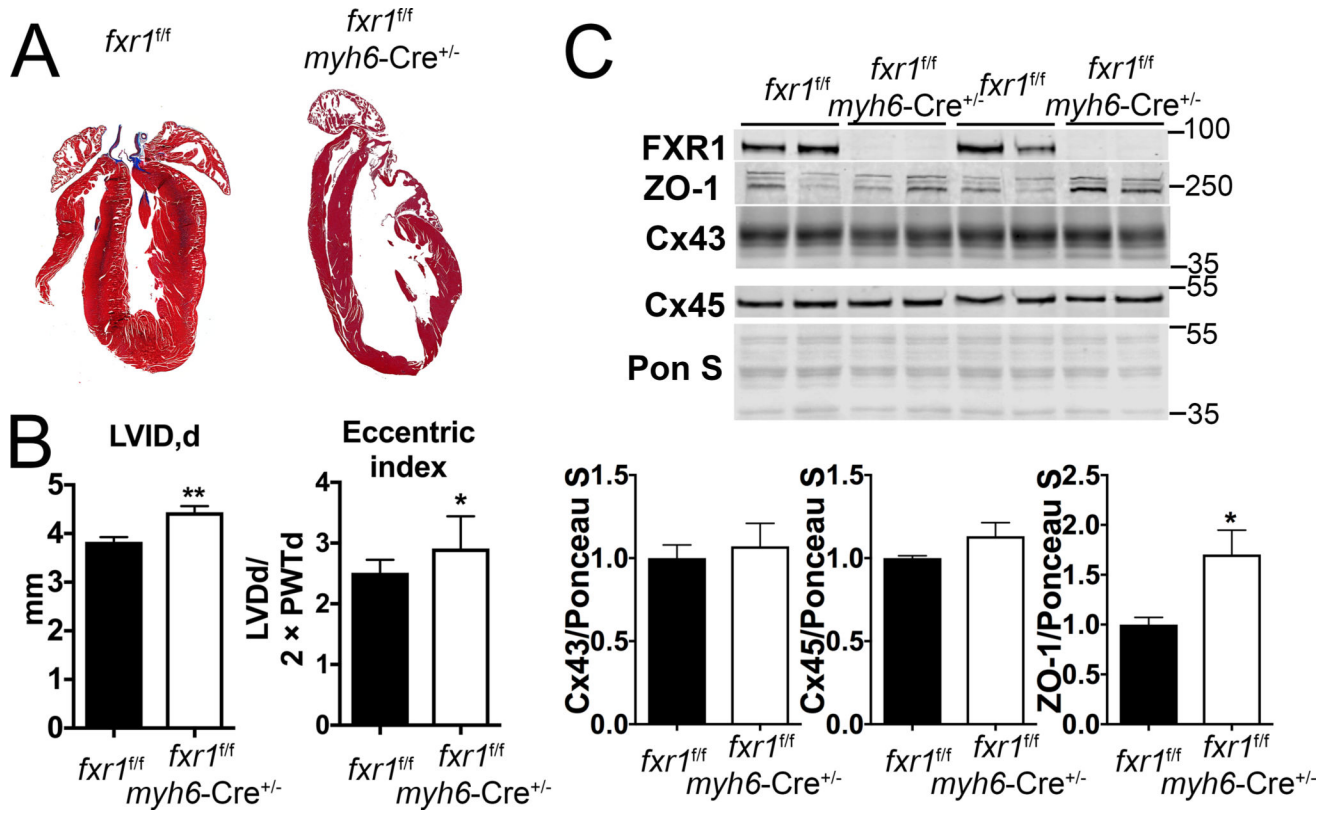


Figure 8. Cardiac-specific loss of FXR1 leads to DCM with no change in Cx43 expression in mice
(A) Longitudinal sections of D56 paraffin-embedded hearts stained with Masson's Trichrome. **(B)** Echocardiography analysis of *fxr1^{fl/fl}* and *fxr1^{fl/fl}Myh6-Cre* hearts at D56. LV end diastolic diameter (*fxr1^{fl/fl}*: 3.831±0.096, *fxr1^{fl/fl}myh6-Cre^{+/-}*: 4.44±0.126 fold increase, p<0.001) and eccentric index (*fxr1^{fl/fl}*: 2.511±0.061, *fxr1^{fl/fl}myh6-Cre^{+/-}*: 2.912±0.152 fold increase, p<0.05) are significantly increased in *fxr1^{fl/fl}Myh6-Cre* mice (n=8) versus *fxr1^{fl/fl}* control (n=8). **(C)** Immunoblots of *fxr1^{fl/fl}* and *fxr1^{fl/fl}Myh6-Cre* left ventricle lysates probed for FXR1, ZO-1, Cx43 and Cx45 plus Ponceau S staining (for actin) of the blot used for normalization. ZO-1 is significantly increased in *fxr1^{fl/fl}Myh6-Cre* (1.703±0.244 fold increase, p<0.05) compared to *fxr1^{fl/fl}* control (1±0.072). Cx43 and Cx45 protein levels are unchanged in *fxr1^{fl/fl}Myh6-Cre* hearts. Students T-test was used to calculate statistical significance: p value *p<0.05, **p<0.01.